Comparative Study of Avalanche Photodiodes with Different Structures in Scintillation Detection[1]

M. Moszyński[a)], *IEEE Member,* M. Kapusta[a)], M. Balcerzyk[a)],
M. Szawlowski[b)], *IEEE Member,* D. Wolski[a)], I. Węgrzecka[c)], M. Węgrzecki[c)],
a) Soltan Institute for Nuclear Studies, PL 05-400 Świerk-Otwock, Poland
b) Advanced Photonix, Inc. 1240 Avenida Acaso, Camarillo, CA 93012, USA
c) Institute of Electron Technology, Al. Lotników 32/46, PL 02-668 Warsaw, Poland

Abstract

The performance of beveled-edge Large Area Avalanche Photodiodes (LAAPD) produced by Advanced Photonix, Inc. (API), Hamamatsu SPL 2560 APDs and APDs from Institute of Electron Technology (ITE) were studied in scintillation detection using CsI(Tl), BGO, LSO and YAP scintillators. Measurements covered DC gain characteristics, relative response to X-rays and light, energy resolution for 5.9 keV X-rays from ^{55}Fe source, determination of electron-hole (e-h) pair number for the studied scintillators and their energy resolution for 662 keV γ-rays from a ^{137}Cs source. The highest number of e-h pairs was measured with the LAAPD from API equal to 33800 e-h/MeV for CsI(Tl) and 10200 e-h/MeV for YAP crystal. In case of the Hamamatsu APD, the respective numbers were 30900 e-h/MeV and 4700 e-h/MeV. For the APD from ITE we measured 16500 e-h/MeV with CsI(Tl). The best energy resolution of 4.9% for 662 keV was observed with CsI(Tl) coupled to LAAPD from API, while the Hamamatsu APD showed somewhat worse result of 5.8%.

I. Introduction

The growing interest in applications of avalanche photodiodes in physics experiments and nuclear medicine prompted recently their intensive study in scintillation detection. Our team [1-6] has studied performance of beveled-edge LAAPDs produced by API. Groups associated with CMS experiment [7-9] at CERN and groups developing PET [10,11] have done much research work on characterization of Hamamatsu APDs. In this paper we perform a precise comparison of properties of both types of APDs measured in the same conditions with typical scintillators.

The studied APDs differ by their internal structure. The beveled-edge LAAPD is made by growing a 12 μm p-type epitaxial layer on n-type neutron transmutation doped (NTD) silicon. Low surface electric field across the junction allows for uniform avalanche breakdown inside the device. Wide depletion layer extends mainly into n-type region resulting in a very low multiplied component of dark current. The profile of the electric field is presented at Fig. 1a. The broad gain region enables device operation at high gain with low excess noise and excellent gain uniformity.

The Hamamatsu APD, model SPL 2560 was chosen for the test because of its large scale application in electromagnetic calorimeter of the CMS detector at CERN The device was optimized for wavelength range below 550 nm and low sensitivity to nuclear counter effect [9]. Only photons absorbed in a thin (<7 μm) p-type layer in front of the junction contribute to electric charge undergoing full multiplication. The presumed electric field profile of this device is shown in Fig. 1b.

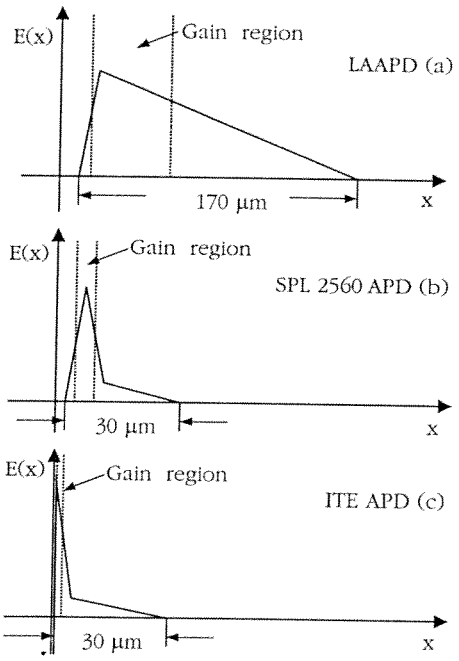

Figure 1: The electric field profile in LAAPD (a), SPL 2560 APD (b) and ITE APD (c).

To better understand observed differences in the performance of studied APDs, the APD produced by ITE, Warsaw, Poland [12] was included in the study. Although this APD was optimized for the detection of near infrared radiation, it is also sensitive to the visible range above 550 nm. The diode of the n^+-p-π-p^+ structure with a guard ring and channel stopper is made from silicon wafer with a π-type, high resistivity epitaxial layer. In result, the sensitive p-region is behind the avalanche region. The front n-type region and avalanche region are made very narrow to reduce the light absorption. Its electric field profile is presented in Fig. 1c.

[1] Support for this work was provided by the Polish Committee for Scientific Research, Grants Nos. 8T 10C 005 15 and 8T 11B 037 13

II. EXPERIMENTAL DETAILS

The basic properties of the studied APDs are collected in Table 1. Note considerably different bias voltages necessary to obtained gain of 100, reflecting different device structures. The LAAPD and APD from ITE were tested windowless. The crystals were glued with silicone grease, directly to the die. The Hamamatsu SPL 2560 APD was sealed in a resin that constitutes a front window.

Table 1
Properties of the studied APDs

Manufacturer	API	Hamamatsu	ITE
Type	394-70-73-500	SPL 2560 (batch 1999)	APD 5 mm 8/8/52/09.99
Size	Ø10 mm	5x5 mm	Ø5 mm
Window	None	Resin	None
Q.E.	77%/400 nm	65%/400 nm	74%/800 nm
Gain	100 at 1741 V	100 at 382 V	100 at 151 V
Dark current	39.5 nA	11.5 nA	66.6 nA
Capacitance	65 pF	117 pF	110 pF
Rise time	10 ns		12 ns

The APDs were studied using 5.9 keV X-rays from ^{55}Fe source, light pulses from laser and LEDs, and with CsI(Tl), BGO, LSO and YAP scintillators. The used laser and LED light sources allowed producing light signals of 670, 560 and 430 nm. This was particularly important in the test of Hamamatsu and ITE APDs. Tested scintillators with the light emission peaks at 560, 490, 420 and 365 nm, respectively, virtually cover the full spectrum of scintillation light.

The size of scintillators allowed full light collection with the APDs. The CsI(Tl) and YAP with dimensions of 5x5x5 mm^3, BGO of 3x3x5 mm^3 and LSO of 4x5x14 mm^3 were selected for the measurements. The ITE device was tested only with CsI(Tl), because of device negligible sensitivity to other crystals peak emission wavelengths. A small mismatch of the square 5x5x5 mm^3 crystal exit and round shape of the 5 mm diode resulting in lowering the measured number of e-h pairs, has to be noted.

In all the experiments the signal from APDs was fed to a preamplifier (Ortec 142AH) and then to a spectroscopy amplifier (Tennelec TC244). A PC-based multichannel analyzer (Tukan) was used to record energy spectra.

III. RESULTS

A. Gain Characteristics, X-rays and Light Detection

Fig.2 presents the DC gain characteristics of SPL 2560 and ITE APDs. In the inset of Fig. 2a, the spread of gain for different wavelengths of light is shown in detail for the Hamamatsu device. The precise measurement of the gain characteristics was important for the further determination of the number of e-h pairs produced by light signals. For the LAAPD the gain characteristic provided by the manufacturer was used.

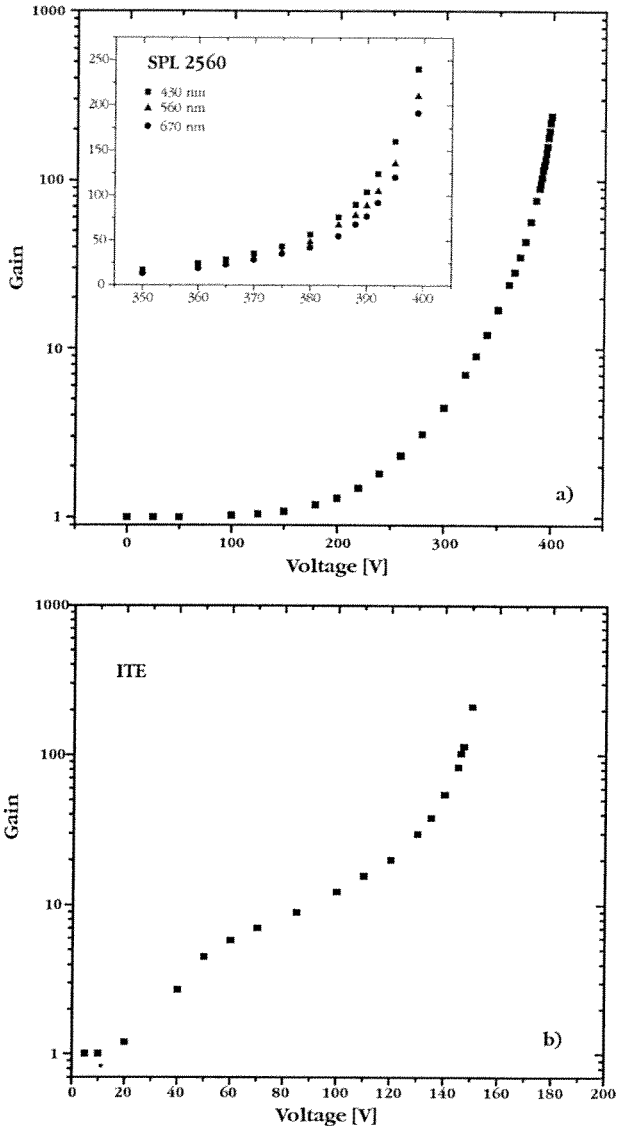

Figure 2: DC gain characteristics of SPL 2560 (a) and ITE (b) APDs. In the inset of (a) the spread of gain for different wavelengths is showing in detail. Error bars are within the size of the points.

Fig. 3 presents energy spectra showing 5.9 keV X-rays, 560 nm light pulser, and test pulser peaks as observed with LAAPD and SPL 2560 APD. The presence of the test pulser peak in the spectra allows for calibration of detected optical signals in energy units or e-h pair numbers, and measurements of APD dark noise and preamplifier noise contributions. Note an excellent energy resolution of the 5.9 keV peak measured with LAAPD. The same peak observed with the Hamamatsu APD is shifted down on energy scale calibrated with the test pulser.

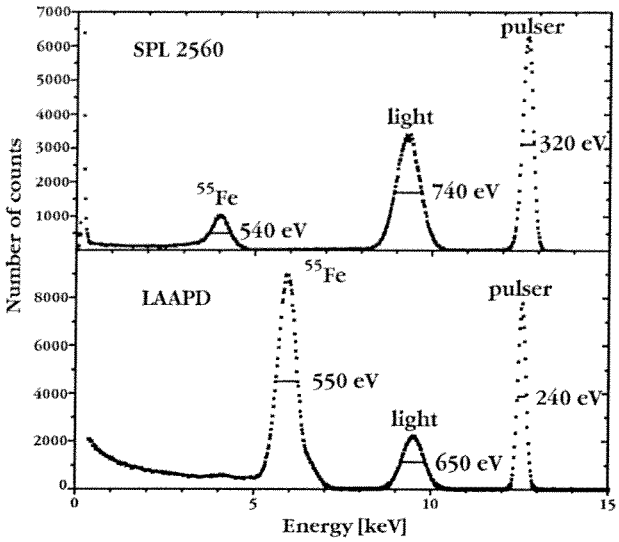

Figure 3: The energy spectra showing 5.9 keV X-rays, and light and test pulser peaks measured with LAAPD (a) and SPL 2560 APD (b).

This effect is clearly seen in Fig. 4 showing the ratio of APD gain for X-rays and light versus gain measured for all the APDs. The measurements were carried out at simultaneous illumination by 5.9 keV X-rays from ^{55}Fe and the light pulse from the LED pulser. Note that only LAAPD produces the same gain for X-rays and light, up to gain of 100, see also [5,6]. For the other APDs, the gain for X-rays is dramatically reduced [7,8], with the increase of the device light gain. The observed effect is evidently associated with the internal structure of APDs.

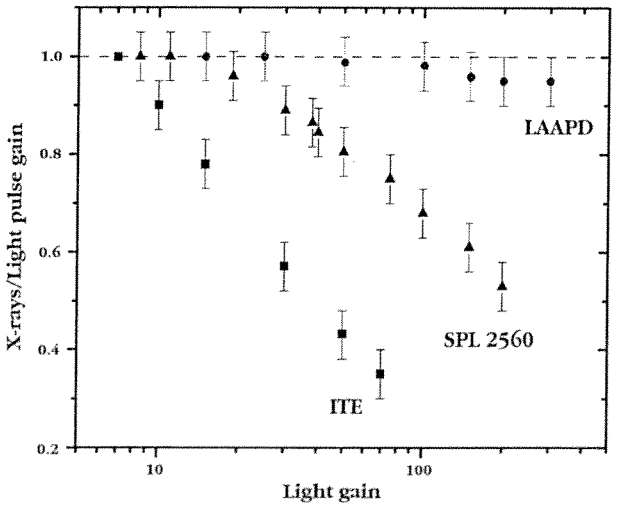

Figure 4: The ratio of the APDs gain for X-rays and light pulses measured for LAAPD, and SPL 2560 and ITE APDs.

The energy resolution of the light pulse detected by APD is limited mainly by the statistics related to avalanche multiplication, statistic of primary e-h pairs and dark noise contribution of the APD-preamplifier system. Assuming Gaussian shape of the detected peak, the energy resolution ΔE of the light pulser peak (expressed in keV), can be described by the following equation:

$$\Delta E^2 = (2.36)^2 \, F \, E \, \varepsilon + \Delta_{noise}^2 \qquad (1)$$

where E is the energy of the light peak in keV, F is the excess noise factor, ε is the energy per e-h pair creation (3.6 eV for silicon), and Δ_{noise} is the dark noise contribution of the diode-preamplifier system (FWHM in keV).

The Eq. (1) allows determination of the excess noise factor for tested APDs, based on the energy resolution of peaks produced by a light pulser (see Fig. 3). Fig. 5 shows the dependency of the excess noise factor versus gain for the tested APDs. To increase the accuracy, all the measurements were carried out at least three times and the average value was plotted. Note the largest excess noise factor for ITE APD. It reflects a very intense and narrow distribution of electric field in the avalanche region (see Fig. 1). For the SPL 2560 APD different curves are observed depending on the wavelength of light. For longer wavelengths, when light may enter into the avalanche region, spread of gain correlated to the depth of interaction increases the excess noise factor. For the API LAAPD and Hamamatsu APD at 430 nm, comparable curves are seen with the excess noise factor below 2 for the gain up to 100.

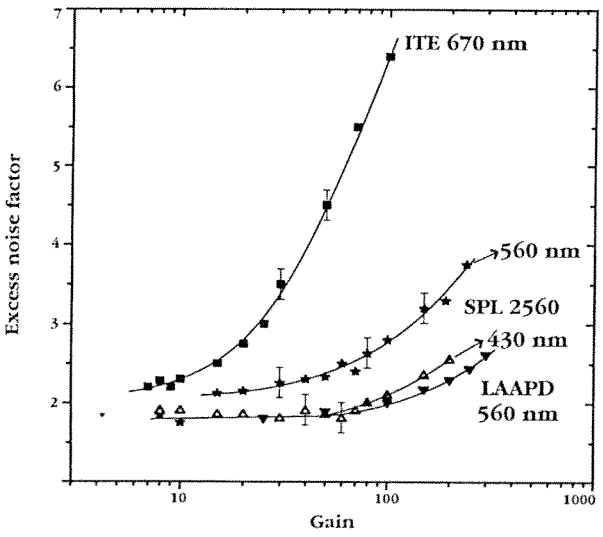

Figure 5: Excess noise factor versus APD gain measured for the tested diodes. Note different characteristics for different light wavelengths observed with the SPL 2560 APD.

B. Scintillation Detection

1) Number of e-h pairs

The same gain for X-rays and light pulses, observed with the LAAPD, allows using the 5.9 keV X-ray peak as a good reference to measure number of e-h pairs. For the other APDs the number of e-h pairs was measured using a reference test pulser, calibrated against X-rays detected in pin photodiode.

Separate gain characteristics measured for the wavelengths close to the peak emission of the crystal were used in each case. Table 2 presents the number of e-h pairs measured for all tested scintillators using different APDs operated at gain of 50. Shaping time constant of 3 μs was used in all the tests.

Table 2
Number of e-h pairs measured for different scintillators

Crystal	LAAPD	SPL 2560	ITE
CsI(Tl)	33800±1700	30900±1600	16500±800
BGO	5200±250	4200±200	-
LSO	19000±1000	8900±450	-
YAP	10200±500	4700±200	-

Note systematically higher numbers of e-h pairs measured with the LAAPD then those for the SPL 2560 APD. The 10% difference observed for CsI(Tl) can be partially explained by the light attenuation introduced by the Hamamatsu device window. Results obtained with other crystals indicate superior quantum efficiency of API devices.

It is worth adding that even for BGO, which peak emission at 490 nm is close to that of PWO crystal, the number of e-h pairs measured with SPL 2560 APD is lower by 20%. In principle, this APD is optimized for the most effective detection of light from PWO crystal. Much lower number of e-h pairs observed with ITE APD is the effect of partial light absorption in the front layer before light reaches the device sensitive region.

2) Energy Resolution

Fig. 6 presents a comparison of energy spectra of 662 keV γ-rays from a ^{137}Cs source measured with 5x5x5 mm^3 CsI(Tl) crystal coupled to LAAPD, and SPL 2560 and ITE APDs.

Note an excellent energy resolution of 4.9% measured with the LAAPD, comparable to that reported previously in Ref. [3] for this type of APDs. The energy resolution measured with SPL 2560 and ITE APDs are too large to be explained entirely by a lower number of e-h pairs. In both cases an additional spread in energy resolution may be explained by the fact that light is detected in APD regions of unequal sensitivity, including the avalanche region. The emission spectrum of CsI(Tl) is wide and it is distributed between 400 and 600 nm. Thus one can expect a different gain for different wavelength components of emitted light.

Energy spectra of 662 keV γ-rays measured with BGO and YAP crystals coupled to LAAPD and SPL 2560 APD are shown in Figs 7 and 8. Note again that a much better energy resolution was measured with the crystals coupled to the LAAPD. This is particularly well pronounced at spectra measured with BGO. Bismuth escape peak is much better separated in the spectrum measured with the LAAPD.

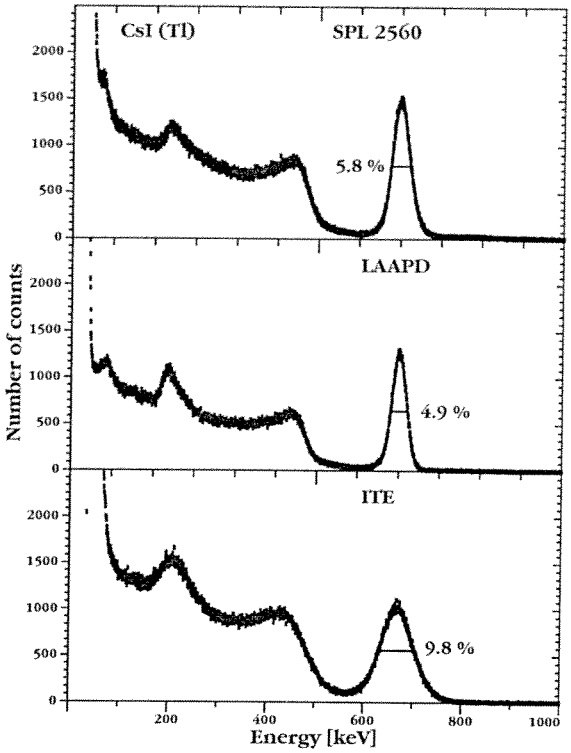

Figure 6: Energy spectra of 662 keV γ-rays from a ^{137}Cs source measured with 5x5x5 mm^3 CsI(Tl) crystal coupled to LAAPD, and SPL 2560 and ITE APDs.

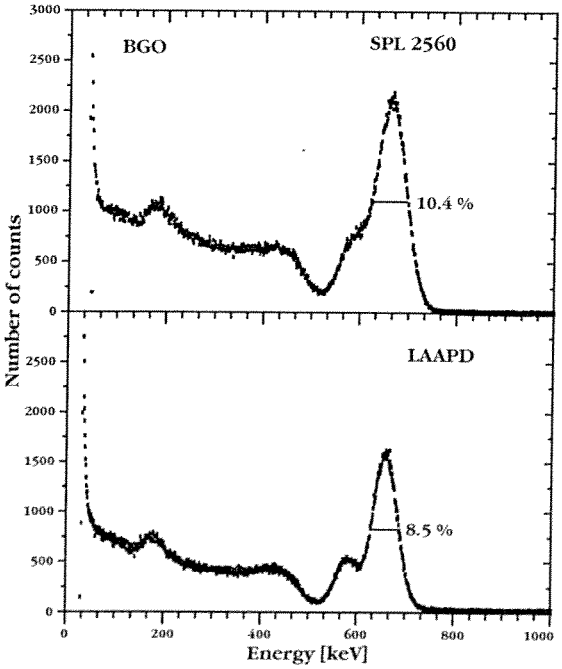

Figure 7: Energy spectra of 662 keV γ-rays from a ^{137}Cs source measured with 5x3x3 mm^3 BGO crystal coupled to LAAPD and SPL 2560 APD.

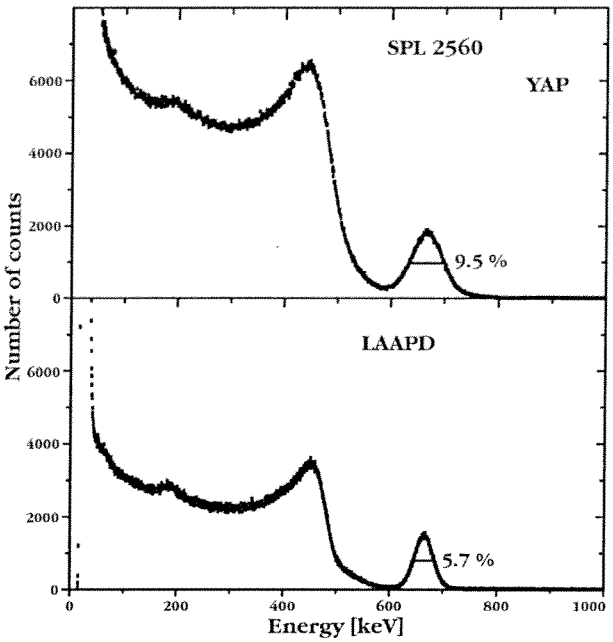

Figure 8: Energy spectra of 662 keV γ-rays from a ^{137}Cs source measured with 5x5x5 mm^3 YAP crystal coupled to LAAPD and SPL 2560 APD.

Table 3 summarizes a comparison of energy resolution measured with different combination of studied crystals and APDs. In each case, device gain and shaping time constant were optimized for the best energy resolution.

Table 3
Energy resolution for 662 keV γ-rays from a ^{137}Cs source measured with different crystals and APDs

Crystal	LAAPD	SPL 2560	ITE
CsI(Tl)	4.9±0.2%	5.8±0.3%	9.8±0.4%
BGO	8.5±0.3%	10.4±0.4%	-
LSO	9.3±0.4%	12.3±0.5%	-
YAP	5.7±0.3%	9.3±0.4%	-

Table 3 shows a regularly better energy resolution measured with the LAAPD than those observed with Hamamatsu APD. For LSO and YAP this can be explained by a significantly higher number of e-h pairs generated by the API device. However, in all the cases the deterioration of energy resolution measured with Hamamatsu APD cannot be explained only by the statistical error and noise contribution.

This effect is better presented in Table 4, where all the components of energy resolution were calculated for the measured spectra, following Ref. [3]. The energy resolution, ΔE/E, of the full energy peak measured with a scintillator coupled to an APD can be expressed as:

$$(\Delta E/E)^2 = (\delta_{sc})^2 + (\Delta N/N_{e\text{-}h})^2 + (\Delta_{noise}/N_{e\text{-}h})^2 \qquad (2)$$

where δ_{sc} is the intrinsic resolution of the crystal, $\Delta N/N_{e\text{-}h}$ represents the statistical contribution and $\Delta_{noise}/N_{e\text{-}h}$ is the dark noise contribution.

Table 4
Energy resolution and its components

Crystal	e-h number[a)]	ΔE/E[a)] [%]	$\Delta N/N_{e\text{-}h}$ [%]	$\Delta_{noise}/N_{e\text{-}h}$ [%]	δ_{sc} [%]
LAAPD					
CsI(Tl)	25800±770	4.9±0.2	2.0±0.03	1.0±0.03	4.3±0.3
BGO	3440±100	8.5±0.3	5.6±0.1	4.7±0.1	4.3±1.2
LSO	12600±380	9.3±0.4	2.9±0.87	0.95±0.03	8.8±0.4
YAP	6750±200	5.7±0.3	4.0±0.1	1.8±0.04	3.6±0.3
SPL 2560 APD					
CsI(Tl)	20500±600	5.8±0.3	2.5±0.03[b)]	1.2±0.04	5.1±0.2
BGO	2430±73	10.4±0.4	6.4±0.1[c)]	4.4±0.1	6.9±0.4
LSO	5900±180	12.3±0.5	4.1±0.1[c)]	1.8±0.04	11.4±0.5
YAP	2900±90	9.3±0.4	5.9±0.1[c)]	3.3±0.08	6.4±0.3
ITE APD					
CsI(Tl)	10900±530	9.8±0.4	4.2±0.1	5.3±0.1	7.1±0.4

a) Measured for 662 keV in optimal test conditions (APD gain and shaping time),
b) F = 2.4 (measured with 560 nm LED),
c) F = 1.8 (measured with 430 nm LED).

In the last column of the Table 4, the intrinsic resolution of crystals calculated from all the measurements is presented. This quantity is, in principle, described by the properties of scintillator and it should be independent of the light sensor [3]. The values found in the measurements with the LAAPD are comparable to those measured previously with another LAAPD and XP2020Q PMT [3]. The intrinsic resolution evaluated from the measurements with SPL 2560 and ITE APDs is much worse, for all the tested crystals, suggesting that an additional spread of signal from both the devices is observed. Note that in the evaluation of intrinsic resolution of scintillators, the essential components of the APD signal dispersion, i.e. the statistical contribution and dark noise have been already excluded, see eq. (2).

In case of the ITE APD, part of light from CsI(Tl) crystal is evidently detected in the avalanche region because of the device structure with the sensitive region located behind the avalanche region. Moreover, the wide emission spectrum of CsI(Tl) introduces an additional spread of gain, which affects the pulse height resolution.

In case of the Hamamatsu SPL 2560 APD, a similar effect may be expected for scintillators with longer wavelengths of emitted light, as CsI(Tl) and BGO. Because of the device narrow sensitive layer, a part of light can be also detected in the avalanche region. Then, a different gain may be observed for different light components. However, this does not explain

the deterioration of the intrinsic resolution observed for LSO and YAP with the peak emission at 420 nm and 365 nm, which have absorption lengths in silicon of approximately of 0.25 μm and 0.015 μm, respectively. For such a short penetration depth, especially in case of YAP, device surface effects (e.g. trapping) can be responsible for significant degradation of measured energy resolution. Lecomte et al [13] observed similar effect in the early versions of Buried Junction APD. Further studies of the Hamamatsu APD are needed to obtained detailed explanation of the device performance.

IV. CONCLUSIONS

The presented study showed that API beveled-edge LAAPD is the most suitable device for scintillation detection. This is confirmed by the highest number of e-h pairs obtained for scintillators with different emission spectra and the highest energy resolution measured for 662 keV γ-rays from a ^{137}Cs source.

The LAAPD is a general purpose APD optimized to detect light in a broad range of wavelengths above 250 nm. Its excellent properties in scintillation detection were also confirmed previously by high energy resolution measured with both, YAP (365 nm) and CsI(Tl) (560 nm) crystals [3,5].

In contrast, the tested SPL 2560 APD from Hamamatsu was optimized for detection of light from PWO, according to the requirements of CMS collaboration [7,8], which resulted in the highest sensitivity at 420 - 490 nm. Also, the width of a front sensitive region was reduced to minimize nuclear counter effect.

In spite of the fact that ITE APD was optimized for near infrared radiation, the device proved to be useful in scintillation detection with CsI(Tl) crystals. These smaller devices would benefit systems where price, compactness and simplicity of the biasing are of primary importance.

V. REFERENCES

[1] M. Moszyński, T. Ludziejewski, D. Wolski, W. Klamra, M. Szawlowski, M. Kapusta, "Subnanosecond Timing with Large Area Avalanche Photodiodes and LSO Scintillators", IEEE Trans. on Nucl. Sci. 43(1996)1298.

[2] M. Moszyński, M. Kapusta, D. Wolski, M. Szawlowski, W. Klamra, "Blue Enhanced Large Area Avalanche Photodiodes in Scintillation Detection with LSO, YAP and LuAP Crystals", IEEE Trans. on Nucl. Sci. 44(1997)436.

[3] M. Moszyński, M. Kapusta, D. Wolski, M. Szawlowski, W. Klamra, "Energy Resolution of Scintillation Detectors Readout with Large Area Avalanche Photodiodes and Photomultipliers", IEEE Trans. on Nucl. Sci. 45(1998)472.

[4] M. Moszyński, M. Kapusta, J. Zalipska, M. Balcerzyk, D. Wolski, M. Szawlowski, W. Klamra, "Low Energy γ-rays Scintillation Detection with Large Area Avalanche Photodiodes", IEEE Trans. on Nucl. Sci. 46(1999)243.

[5] M. Moszyński, M. Kapusta, M. Balcerzyk, M. Szawlowski, D. Wolski, "Large Area Avalanche Photodiodes in X-rays and Scintillation Detection", Nucl. Instr. Meth. A442(2000)230.

[6] M. Moszyński, M. Szawlowski, M. Kapusta, M. Balcerzyk, D. Wolski, „Large Area Avalanche Photodiodes in X-rays and Light Detection", IEEE Trans on Nucl. Sci., in press.

[7] J.P. Pansart, "Avalanche Photodiodes for particle detection", Nucl. Instr. Meth., A387(1997)186.

[8] A. Karar, Y. Musienko, J.Ch. Vanal, „Characterisation of avalanche photodiodes for calorimetry applications", Nucl. Instr. Meth. A428(1999)413.

[9] K. Deiters, Y. Musienko, S. Nicol, B. Patel, D. Renker, S. Reucroft, R. Rusack, T. Sakhelsshivi, J. Swain, P. Vikas, "Properties of the most recent avalanche photodiodes for the CMS electromagnetic calorimeter", Nucl. Instr. Meth. A442(2000)193.

[10] B. Pilcher, G. Boning, E. Lorenz, R. Mirzoyan, W. Pimpl, M. Schwaiger and S.I. Ziegler, "Studies with a Prototype High Resolution PET Scanner Based on LSO-APD Modules", IEEE Trans. on Nucl. Sci. 45(1998)1298.

[11] Ruru Chen, A. Fremout, S. Tavernier, P. Bruyndonckx, D. Clement, J.-F. Loude, C. Morel, "Readout of scintillation light with avalanche photodiodes for positron emission tomography", Nucl. Instr. Meth. A433(1999)637.

[12] I. Wegrzecka, M. Wegrzecki, „The properties of ITE's silicon avalanche photodiodes within the spectral range used in scintillation detection", Nucl. Instr. Meth. A426(1999)212.

[13] R. Lecomte, C. Pepin, D. Rouleau, H. Dautet, R.J. McIntyre, D. McSween, P. Webb, "Radiation detection measurements with a new Buried Junction silicon avalanche photodiode", Nucl. Instr. Meth. A423(1999)92.